PRAMANA
—journal of
physics

© Printed in India

Vol. 50, No. 3,
March 1998
pp. 239–251

Third harmonic generation in layered media in presence of optical bistability of the fundamental

JOLLY JOSE and S DUTTA GUPTA
School of Physics, University of Hyderabad, Hyderabad 500 046, India
email: sdgsp@uohyd.ernet.in

MS received 23 February 1998

Abstract. We study third harmonic generation in layered configuration when the fundamental exhibits bistable response. We consider two geometries, namely, a Fabry–Perot cavity with reflection coatings and a distributed feedback structure with alternate nonlinear layers. In both the cases for suitable choice of frequency, the power response at the fundamental frequency is bistable. We show that bistability of the fundamental leads to a multivalued character of the generated third harmonic in both the forward and backward directions. Moreover, we study frequency response in the case of the Fabry–Perot cavity and show that additional structures arise in the generated third harmonic due to frequency bistability of the fundamental. Our calculations suggest the possibility of an all optical switch at third harmonic frequency controlled by the parameters (like intensity, frequency) of the fundamental.

Keywords. Layered media; third harmonic generation; optical bistability.

PACS No. 42.65

1. Introduction

Harmonic generation in layered or periodically modulated media has been drawing considerable attention [1–3]. It has been well known that the nonlinear processes in various materials can be enhanced by using suitable geometries. Resonances and the associated local field enhancements have been utilized to lower the threshold for nonlinear processes and increase their efficiency. To this end high quality factor (high Q) modes of a Fabry–Perot cavity or a distributed feedback structure as well as surface and guided modes have been exploited [4–11]. Use of the reflection coatings in Fabry–Perot cavities leads to such high Q modes [10]. In finite distributed feedback structures such modes arise at the edge of the Bragg rejection bands [12, 13]. Optical bistability and multistability using such modes have been theoretically demonstrated [8]. Very recently there has been a lot of interest in harmonic generation using distributed feedback structures [2, 3]. Bethune has developed a matrix method to calculate the generated third harmonic in the forward and backward directions in a multilayered sample [2]. The method is restricted to the case in which the nonlinear process is weak in the sense that the specified pump waves are essentially unaffected by the nonlinear processes. Very recently, based on Bethune's analysis, it was shown that the local field enhancement aspect of the periodic structure can be exploited to enhance the

generated harmonics [11]. It was observed that there exists an enhancement in the generated third harmonic when the fundamental frequency matches one of the mode frequencies of the distributed feed back structure. The observed feature was due to the local field enhancement for the fundamental. Since the fundamental determines the source for the third harmonic, an enhancement in the fundamental distribution leads to a corresponding enhancement in the generated harmonic. However, in all these studies the bistable behavior of the fundamental which is crucial near a resonance was neglected. Because of large local field enhancement the self action of the fundamental can not be neglected. It is thus necessary to reexamine the harmonic generation process when there is allowance for this self action leading to the bistability of the fundamental. In this paper we study third harmonic generation in cavities supporting high Q-modes where the bistable behavior of the fundamental is taken into account. We consider two types of cavity configurations, namely, Fabry–Perot cavity with reflection coatings and a distributed feedback cavity with alternating linear and nonlinear slabs. We assume that the generation of the third harmonic does not deplete the pump though we include nonlinear response of the fundamental. In other words, third harmonic wave does not affect the fundamental but bears the signature of the bistable response at the fundamental frequency. We show that the third harmonic also shows bistable behavior in the same domain as the fundamental. Our studies suggest that one may possibly devise a switch at the third harmonic frequency which is controlled by the fundamental intensity or frequency. In all our calculations due to lack of dispersion data for the media considered, we were forced to assume the media to be dispersionless. Hence we could not incorporate the phase-matching aspects of harmonic generation. With the availability of dispersion data the periodic structure can be designed to incorporate quasi phase-matching leading to better harmonic output [14, 15].

The organization of the paper is as follows: In § 2 we present the mathematical formulation and recall some of the results pertaining to optical bistability in layered media. In § 3 we present the results of our numerical investigations for both the systems, namely, Fabry–Perot and distributed feedback cavities and in § 4, we conclude the paper.

2. Mathematical formulation

Let us consider a stratified medium consisting of linear and nonlinear slabs with linear refractive indices n_l and n_n and widths d_l and d_n, respectively. As mentioned in the introduction, we assumed the media to be dispersionless though dispersion can be incorporated in a trivial fashion. The nonlinearity is assumed to be cubic in nature. The composite medium is embedded in a linear medium with refractive index n_i. Let z be the direction of propagation for a y-polarized electromagnetic wave at frequency ω, normally incident on the left edge of the system. Since the nonlinear medium is assumed to be isotropic a y-polarized fundamental leads to a nonlinear polarization also along y direction. The total nonlinear polarization induced in a nonlinear slab can be written as

$$P_{\mathrm{NL}} = \chi^{(3)}(E_\omega \mathrm{e}^{-i\omega t} + E_{3\omega}\mathrm{e}^{-i3\omega t} + \mathrm{c.c.})^3 \approx P_\omega \mathrm{e}^{-i\omega t} + P_{3\omega}\mathrm{e}^{-i3\omega t} + \mathrm{c.c.} \quad (1)$$

with

$$P_\omega = \chi^{(3)}(3|E_\omega|^2 E_\omega + 3E_\omega^{*2} E_{3\omega} + 6|E_{3\omega}|^2 E_\omega), \tag{2}$$

$$P_{3\omega} = \chi^{(3)}(E_\omega^3 + 6|E_\omega|^2 E_{3\omega} + 3|E_{3\omega}|^2 E_{3\omega}), \tag{3}$$

where E_ω and $E_{3\omega}$ are the electric fields at the fundamental and generated third harmonic frequencies, respectively. In writing eq. (1) we ignored the frequency dependence of $\chi^{(3)}$. We also ignore the effects of higher order harmonics. Henceforth we neglect the effect of third harmonic on the fundamental assuming $|E_{3\omega}| \ll |E_\omega|$. Hence the propagation equations for the fundamental inside the nonlinear slab becomes

$$\frac{d^2\tilde{E}_\omega}{d\tilde{z}^2} + n_n^2 \tilde{E}_\omega = -3|\tilde{E}_\omega|^2 \tilde{E}_\omega, \tag{4}$$

where, we have introduced the dimensionless quantities: $\tilde{z} = k_0 z$ and $\tilde{E}_\omega = \sqrt{4\pi\chi^{(3)}} E_\omega$. As mentioned earlier, in eq. (4) we retained only the term leading to bistability which is crucial near resonance. The equations at 3ω can be written as

$$\frac{d\tilde{E}_{3\omega}}{d\tilde{z}} = 3i(-\tilde{H}_{3\omega}), \tag{5}$$

$$\frac{d(-\tilde{H}_{3\omega})}{d\tilde{z}} = 3i[n_n^2 \tilde{E}_{3\omega} + \tilde{E}_\omega^3 + 3|\tilde{E}_{3\omega}|^2 \tilde{E}_{3\omega} + 6|\tilde{E}_\omega|^2 \tilde{E}_{3\omega}], \tag{6}$$

where $\tilde{E}_{3\omega} = \sqrt{4\pi\chi^{(3)}} E_{3\omega}$. A similar scaling has been used for $\tilde{H}_{3\omega}$.

In what follows, we recall the transfer matrix method used to study the propagation characteristics of the fundamental for linear and nonlinear media. For a linear layer the corresponding characteristic matrix is well known [16]. The tangential components of the electric and magnetic fields, at the right and left of the linear slab, at any frequency can be related by means of this characteristic matrix. As we have neglected the effect of dispersion in our system, the structure of this transfer matrix assumes the same form (except for the wave vector) for both the fundamental as well as the third harmonic. The propagation characteristics of the fundamental and the third harmonic inside a nonlinear slab are studied separately. As far as the fundamental is concerned the nonlinear transfer matrix method is applied [10]. Here we recall only the essential steps. The characteristic matrix of the nonlinear slab depends on the intensities of the forward and backward waves in that medium. The solutions of the fundamental wave equation (eq. (4)) for any jth nonlinear slab can be written as [5, 10]

$$\tilde{E}_{\omega j} = A_{+j} e^{i n_{+j} \tilde{z}} + A_{-j} e^{-i n_{-j} \tilde{z}}, \tag{7}$$

where A_{+j} and A_{-j} are the forward and backward wave amplitudes respectively and n_{+j} and n_{-j} are defined as

$$n_{+j} = n_n[1 + 3(|A_{+j}|^2 + 2|A_{-j}|^2)]^{1/2},$$

$$n_{-j} = n_n[1 + 3(|A_{-j}|^2 + 2|A_{+j}|^2)]^{1/2}. \tag{8}$$

The characteristic matrix which relates the tangential field components at the right and left edge of the nonlinear slab of thickness d_n can be written in terms of n_{+j} and

n_{-j} as

$$M_j = \frac{1}{(n_{+j}+n_{-j})}\begin{bmatrix} n_{+j}\,e^{in_{+j}d_n} + n_{-j}\,e^{-in_{-j}d_n} & -(e^{in_{+j}d_n} - e^{-in_{-j}d_n} \\ -n_{+j}n_{-j}(e^{in_{+j}d_n} - e^{-in_{-j}d_n}) & n_{+j}\,e^{in_{+j}d_n} + n_{-j}\,e^{-in_{-j}d_n} \end{bmatrix}. \quad (9)$$

The knowledge of the fundamental in the nonlinear slab is used to evaluate the source terms in eqs (5) and (6). The propagation equations for the third harmonic (eqs (5) and 6)) are solved numerically after the distribution of the fundamental in the layers is obtained. From the knowledge of the tangential components of the generated third harmonic at the right edge of any jth nonlinear slab one can obtain the components at the left edge by numerically integrating eqs (5) and (6) along the length of the slab.

We start our calculations from the right end of the whole system. We treat the transmitted fundamental amplitude as a parameter. For a given value of the transmitted fundamental amplitude we propagate the fundamental wave from right to left by using the characteristic matrix for linear and nonlinear slabs. The total characteristic matrix, M, for the entire system is written in terms of the characteristic matrices of each layer. Then the incident (A_{in}) and reflected (A_r) amplitudes of the fundamental wave in the medium of incidence can be written in terms of amplitude (A_t) of the medium in which the wave is transmitted as follows

$$\begin{pmatrix} A_{in} \\ A_r \end{pmatrix} = \frac{1}{2n_i}\begin{pmatrix} n_i & 1 \\ n_i & -1 \end{pmatrix} M \begin{pmatrix} 1 \\ n_i \end{pmatrix} A_t. \quad (10)$$

The transmission coefficient for the composite medium at fundamental frequency is given in terms of the elements, m_{ij} of M as

$$T = \left| \frac{2n_i}{(m_{11} + m_{12}n_i)n_i + (m_{21} + m_{22}n_i)} \right|^2. \quad (11)$$

In the case of the third harmonic our calculation starts with a guessed value of transmitted third harmonic amplitude at any transmitted fundamental amplitude. As we did in the case of fundamental, we propagate back the third harmonic wave by calculating the field components at each interface of the system. In the case of linear slabs characteristic matrix approach and for nonlinear slabs the corresponding numerical solutions are used. We then express the incident and reflected third harmonic amplitudes in the medium of incidence in terms of this guessed value of transmitted amplitude. As there is no incident third harmonic, we obtain an expression of the form

$$\tilde{A}_{in} = f(\tilde{A}_t, A_t, \omega) = 0, \quad (12)$$

where $\tilde{A}_{in}(\tilde{A}_t)$ is the incident (transmitted) third harmonic. Equation (12) is solved for $\tilde{A}_t$ for a given A_t which leads to an unique A_{in}. Thus, the solution of eq. (12) leads to the generated transmitted ($\tilde{A}_t$) and reflected ($\tilde{A}_r$) for null input at 3ω.

It was mentioned in the introduction that one has to have cavities supporting high-Q modes in order to have low-threshold nonlinear optical phenomena. We have considered two types of cavity configurations supporting high-Q modes, namely, (a) Fabry–Perot cavity with reflection coatings and (b) distributed feed back cavity with alternating linear and cubic nonlinear slabs. In the following section we explain the above two cavity configurations and obtain the transmitted wave amplitudes for fundamental as well for generated third harmonic.

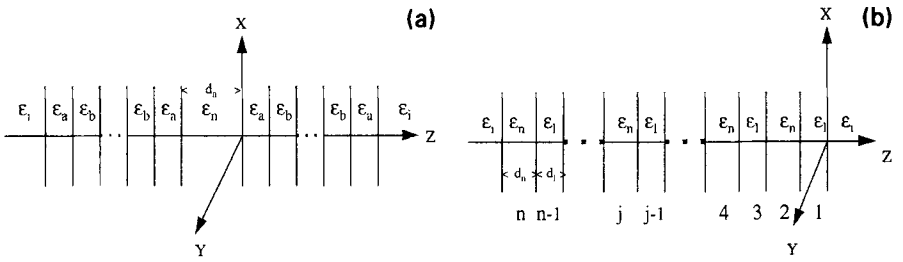

Figure 1. Schematic view of (**a**) Fabry–Perot cavity with reflection coatings with medium parameters $\varepsilon_a = 5.29$, $\varepsilon_b = 1.71$, $\varepsilon_n = 2.5408$ and $\varepsilon_i = 1$ and (**b**) distributed feedback structure with alternating linear and nonlinear slabs with medium parameters $\varepsilon_l = 1.71$, $\varepsilon_n = 2.5408$, $\varepsilon_i = 1$, $d_l = 0.25\lambda$ and $n = 2m = 40$.

2.1 *Fabry–Perot cavity with reflection coatings*

It is well understood that the airy resonances of a Fabry–Perot cavity can be made narrower by increasing the mirror reflectivities. Here we study a composite medium (see figure1a) with one nonlinear slab of linear dielectric constant ε_n, coated on both sides by alternating m low-index (ε_b) and $m+1$ high-index (ε_a) $\lambda/4$ slabs. The initial and final media are linear with the same material of dielectric constants ε_i.

For any transmitted fundamental amplitude (A_t) the forward (A_+) and backward (A_-) amplitudes inside the nonlinear slab can be written as

$$\begin{pmatrix} A_+ \\ A_- \end{pmatrix} = \frac{1}{n_+ + n_-} \begin{pmatrix} n_- & 1 \\ n_+ & -1 \end{pmatrix} M_l \begin{pmatrix} 1 \\ n_i \end{pmatrix} A_t, \tag{13}$$

where M_l is the linear characteristic matrix for the reflection coatings [10]. The above coupled equations along with eq. (8) are solved by using fixed point iteration method to obtain the characteristic matrix M_n of eq. (9). The total characteristic matrix M is then calculated as $M_l M_n M_l$ for the entire system. Using eq. (10) one can then obtain the incident amplitude (A_{in}) and the transmission coefficient T at the fundamental frequency.

For a guessed value of third harmonic amplitude ($\tilde{A}_t$) at the medium of transmittance, the third harmonic tangential field components at the right edge of the nonlinear slab can be written as

$$\begin{pmatrix} \tilde{E}_{3\omega} \\ -\tilde{H}_{3\omega} \end{pmatrix}_{z=0} = M_l \begin{pmatrix} 1 \\ n_i \end{pmatrix} \tilde{A}_t. \tag{14}$$

We integrate the propagation eqs (5) and (6) along the width d_n of the nonlinear slab making use of the knowledge of the distribution of the fundamental amplitudes in order to get the field components at $z = -d_n$. Then the third harmonic incident ($\tilde{A}_{in}$) and reflected ($\tilde{A}_r$) amplitudes in terms of $\tilde{A}_t$ is written as

$$\begin{pmatrix} \tilde{A}_{in} \\ \tilde{A}_r \end{pmatrix} = \frac{1}{2n_i} \begin{pmatrix} n_i & 1 \\ n_i & -1 \end{pmatrix} M_l \begin{pmatrix} \tilde{E}_{3\omega} \\ \tilde{H}_{3\omega} \end{pmatrix}_{z=-d} \tag{15}$$

We now demand that $\tilde{A}_{in} = 0$ and solve the above equation numerically for $\tilde{A}_t$ and get the third harmonic reflected and transmitted amplitudes.

2.2 *Distributed feedback cavity*

Here the arrangement of the slabs is with m periods where each period is with one nonlinear slab and one linear slab of dielectric constants ε_n and ε_l respectively. The schematic view of the system is shown in figure 1b where we have numbered the layers from right to left. The distributed feedback structure is characterized by sharp resonances at the edges of the Bragg bands and we analyse the system behavior by choosing the operating point close to one of these resonances (see point R in figure 6). As all the layers with odd indices are linear the corresponding characteristic matrix can be evaluated in a straightforward way. In any jth slab (with j even) one has to solve the coupled nonlinear equation

$$\begin{pmatrix} A_{j+} \\ A_{j-} \end{pmatrix} = \frac{1}{n_{j+} + n_{j-}} \begin{pmatrix} n_{j-} & 1 \\ n_{j+} & -1 \end{pmatrix} M_{j-1} M_{j-2} \cdots M_1 \begin{pmatrix} 1 \\ n_i \end{pmatrix} A_t, \tag{16}$$

for any transmitted fundamental amplitude A_t which yields the characteristic matrix M_j at fundamental frequency for the jth layer. Thus the total characteristic matrix M for the entire system at fundamental frequency can be obtained as $M_n M_{n-1} M_{n-2} \cdots M$ where $n = 2m$ is the total number of layers. Once M is calculated for the entire system the amplitudes in the layer of incidence and the transmission coefficient are obtained as in the case of Fabry–Perot cavity as explained in the previous section.

In the case of the generated third harmonic wave we propagate the field amplitudes from one period as outlined earlier. In each nonlinear medium we use the corresponding fundamental amplitude while solving the propagation equations. Thus the third harmonic incident ($\tilde{A}_{in}$) and reflected ($\tilde{A}_r$) amplitudes in the medium of incidence is written for any guessed value of the total transmitted third harmonic amplitude ($\tilde{A}_t$) as

$$\begin{pmatrix} \tilde{A}_{in} \\ \tilde{A}_t \end{pmatrix} = \frac{1}{2n_i} \begin{pmatrix} n_i & 1 \\ n_i & -1 \end{pmatrix} \begin{pmatrix} \tilde{E}_n \\ -\tilde{H}_n \end{pmatrix}, \tag{17}$$

where $\tilde{E}_n$ and $\tilde{H}_n$ are the tangential components at the left edge of the nth layer. As we have explained before the roots of the above equation with the condition $\tilde{A}_{in} = 0$ gives the generated third harmonic reflected and transmitted amplitudes.

3. Numerical results and discussion

In this section we present the results of our numerical investigation separately for the cases of Fabry–Perot and distributed feedback cavities.

3.1 *Fabry–Perot cavity with reflection coatings*

In the case of the Fabry–Perot cavity we have chosen the system parameters as, $\varepsilon_n = 2.5408$, $\varepsilon_a = 5.29$ and $\varepsilon_b = 1.71$. The initial and final media are considered to be vacuum with $\varepsilon_i = 1$. The optical width of the nonlinear medium is taken to be $k_0 d_n \sqrt{\varepsilon_n} = 2(1 - \Delta)\pi$ where $\Delta = 0.018$ is the dimensionless resonance half-width. We have chosen the operating point in such a way that the system is detuned slightly by an amount $-2\Delta\pi$ from the peak position of the resonance. In figure 2 we have reproduced the bistability

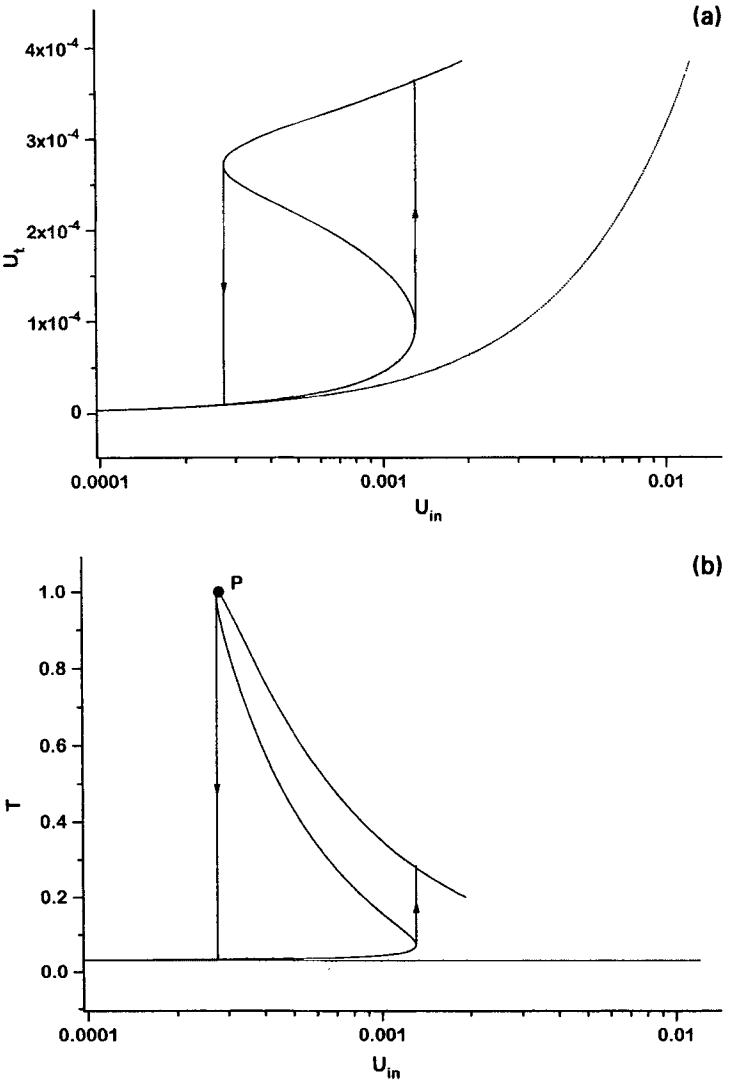

Figure 2. Fundamental (**a**) transmitted intensity U_t and (**b**) transmission coefficient T as functions of fundamental incident intensity U_{in} for $k_0 d_n \sqrt{\epsilon_n} = 2\ (1 - \Delta)\pi$ with $\Delta = 0.018$. Solid (dotted) curve is with (without) self action of the fundamental. The other parameters are as in figure 1a.

features at the fundamental frequency. In figure 2a,b we have plotted transmitted fundamental intensity, $U_t = |A_t|^2(T)$ as a function of incident fundamental intensity, $U_{in} = |A_{in}|^2$. The dotted curve in figures 2a and 2b shows the linear behavior of the system for the same system parameters.

The behavior of the transmitted third harmonic corresponding to the fundamental behavior in figure 2a is depicted in figure 3a, where we have plotted transmitted third harmonic intensity, $\tilde{U}_t = |\tilde{A}_t|^2$ as a function of U_{in}. It is clear from the figure that the third harmonic also exhibits bistable behavior in the same domain as the fundamental. The

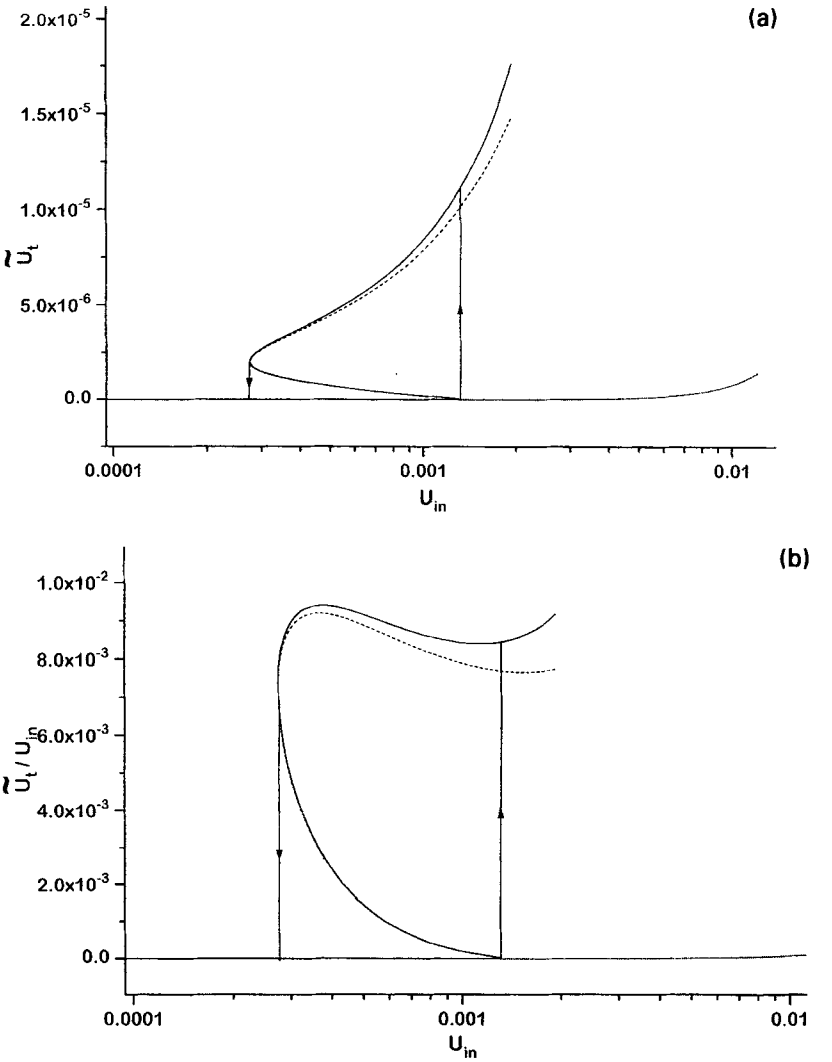

Figure 3. (**a**) Third harmonic transmitted intensity $\tilde{U}_t$ and (**b**) $\tilde{U}_t/U_{in}$ as functions of U_{in}. Solid (dotted) is with (without) self action at ω. The dashed curve gives the result when self action at 3ω is ignored. The parameters of the cavity are as in figure 2.

dotted curve shows the third harmonic output when nonlinear response of fundamental is ignored. The dashed curve explains the system behavior where we have neglected the self action terms of the third harmonic in the propagation equation (i.e., $3|\tilde{E}_{3\omega}|^2\tilde{E}_{3\omega}$ in eq. (6)). It is clear from the curve that the self action effects at 3ω are prominent only for higher values of incident fundamental intensity. Figure 3b shows the dependence of $\tilde{U}_t/\tilde{U}_{in}$ as function of U_{in}. It is clear from figures 2 and 3 that generated third harmonic can be switched from low to high (high to low) values simply by changing the fundamental intensity. Thus one can have an efficient switch at third harmonic frequency which is controlled by the fundamental.

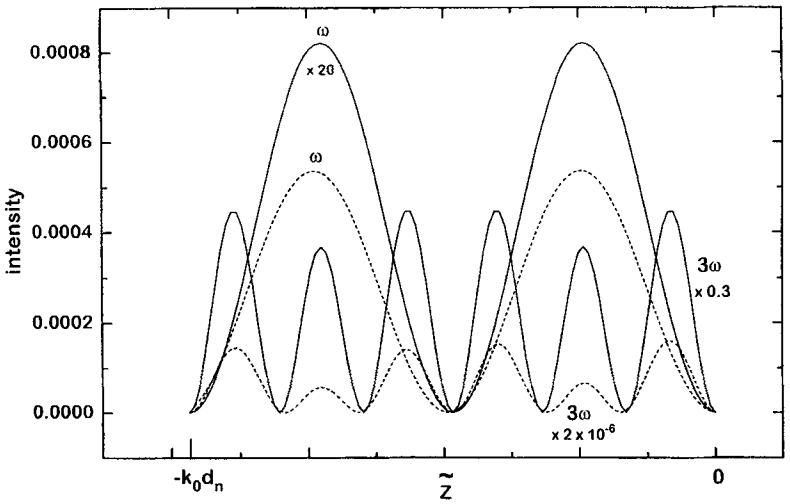

Figure 4. Intensity distribution along the length of the nonlinear slab of the Fabry–Perot cavity of figure 1a where electric field intensities at ω and 3ω are plotted as a function of $\tilde{z}$. The solid (dashed) curve gives our (Bethune's) results. Various curves are labeled by their corresponding frequencies. Note also the different scale factors for various curves.

In order to have a better understanding of the harmonic generation process and to make contact with Bethune's approach we study the field distribution at fundamental and third harmonic frequencies along the length of the nonlinear material. Note that Bethune's results can be recovered from our general results by setting the right hand side of eq. (4) to zero. In other words when there is no self action of the fundamental we have standard plane standing waves at the fundamental frequency the distribution of which determines the generated third harmonic. The results corresponding to the peak of the transmission (see point P in figure 2b which corresponds to $k_0 d_n = 3.8708$, $U_{\text{in}} = 2.7402 \times 10^{-4}$, $U_{\text{t}} = 2.71 \times 10^{-4}$) are shown in figure 4. The solid (dashed) curves give the results for our (Bethune's) approach. We have plotted the electric field intensity $|E(\tilde{z})|^2$ as a function of $\tilde{z}$. Various curves are labeled by the corresponding frequency. Note also the scale factor for the third harmonic. It is clear from figure 4 that there can be drastic differences between our results and those where bistable effects at fundamental are ignored. In fact, the value of $k_0 d_n = 3.8708$ corresponds to an operating point which is away from the linear resonance at the fundamental frequency. Thus one has a low transmission, namely $U_{\text{t}} = 9.71 \times 10^{-6}$ for the same value of U_{in} (see the dotted curve in figure 4). As a consequence the field distribution ignoring the bistable effects is much weaker compared to the case where we allow for the nonlinear resonance. The fundamental distribution gets reflected in the strength of the generated third harmonic. One gets a much stronger third harmonic when such nonlinear resonances are taken into account. It is thus clear that while operating near high-Q modes one has to exercise great care and take into account the self action of the wave which can lead to an altogether different result.

We now turn to the frequency response for a fixed fundamental input. The frequency response of the nonlinear Fabry–Perot cavity is known to exhibit bends in the airy resonances towards left or right 'depending on the sign of the nonlinearity [9]. Bending of

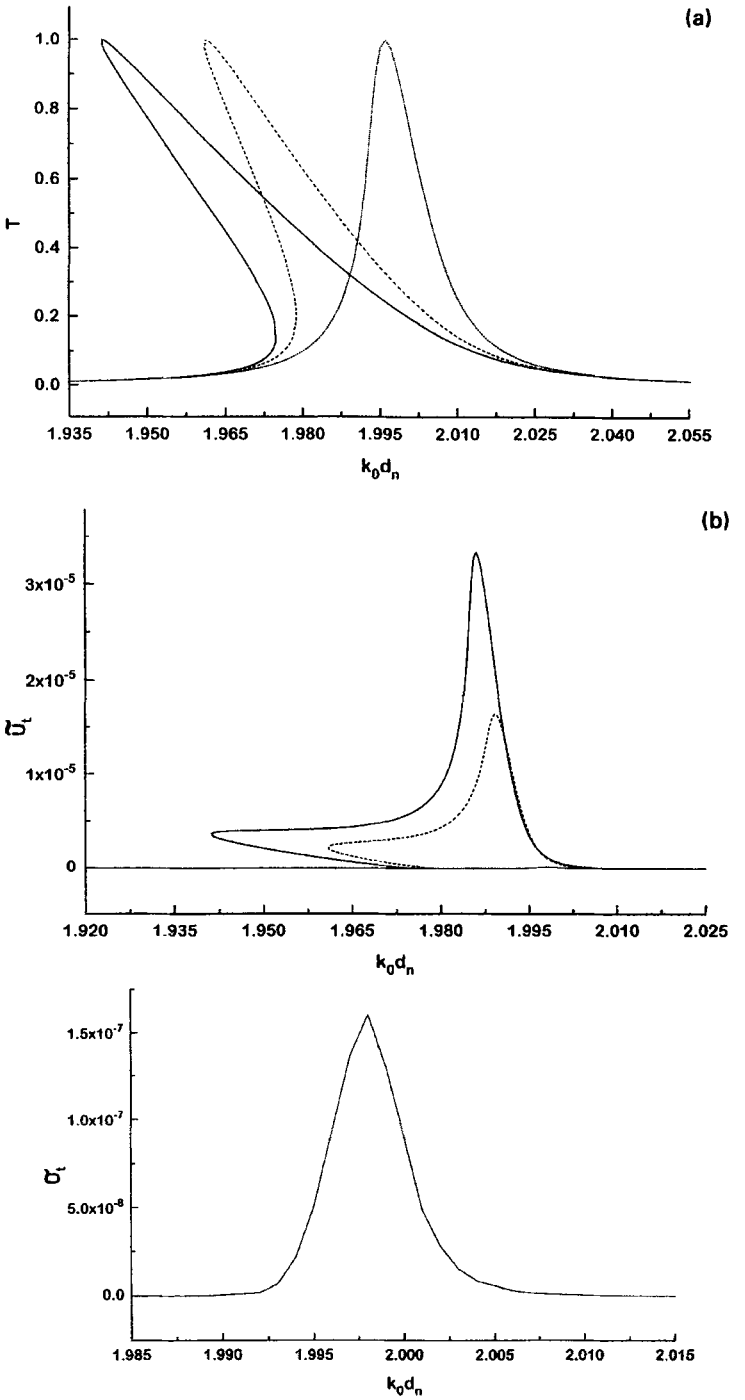

Figure 5. (**a**) Fundamental transmission T and (**b**) transmitted third harmonic intensity $\tilde{U}_t$ for a Fabry–Perot cavity as functions of k_0d_n for three different values U_{in}, namely, $U_{in}=3\times10^{-5}$ (dotted), 3×10^{-4} (dashed) and 4.7×10^{-4} (solid). Inset shows the dotted curve with a different vertical scale. Other parameters are as in figure 1a.

the resonance curves eventually leads to hysterisis loops in the transmission. These features are shown in figure 5a where we have plotted transmission coefficient for three values of incident fundamental intensity, namely, $U_i = 3 \times 10^{-5}$ (dotted curve), 3×10^{-4} (dashed curve) and 4.7×10^{-4} (solid curve). The corresponding results for third harmonic are shown in figure 5b. Since the value of the generated third harmonic for $U_i = 3 \times 10^{-5}$ is very small, the dotted curve appears almost flat compared to other curves in figure 5b. Inset to figure 5b shows this output with a different vertical scale. It is clear from figure 5b that for low fundamental input intensities the response at 3ω does not exhibit bistability (see inset to figure 5b). The situation is different when the input is raised to higher values. The response now becomes multivalued depending on the frequency of the fundamental. Moreover, there is a shift of the resonance locations towards left with an increase in the fundamental input. Note that again we have control over the third harmonic intensity by manipulating the fundamental characteristics like frequency.

3.2 *Distributed feedback cavity*

In the case of distributed feedback cavity we considered the superlattice structure consisting of $m = 20$ periods with vacuum on both sides. The values of ε_n and ε_l are 2.5408 and 1.71, respectively. The thickness of each linear slab is taken to be 0.25λ. Figure 6 shows the linear transmission curve at ω for the system and it shows sharp resonances at the edges of the Bragg band. One is likely to obtain enhanced nonlinear effects making use of these resonances. For further analysis we have chosen the operating point close to one of these resonances (see the point R in figure 6) where the optical thickness of each nonlinear slab is taken to be $k_0 d_n \sqrt{\varepsilon_n} = 1.391\pi$. Figure 7a, b shows the bistable response for the fundamental (third harmonic) as functions of incident

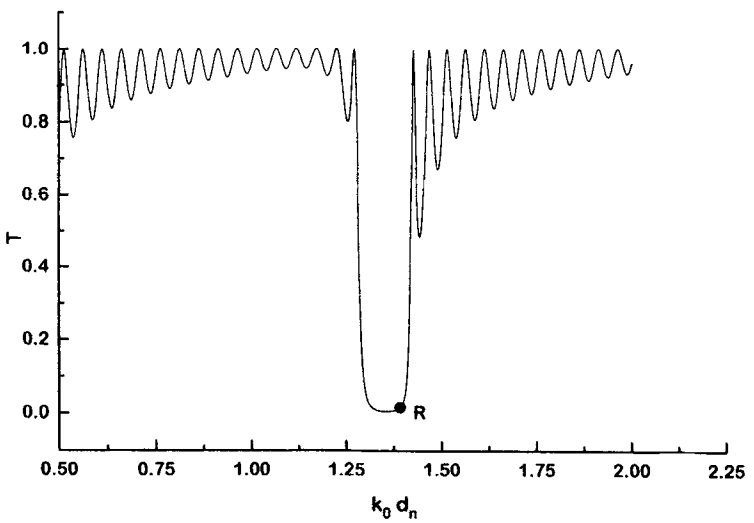

Figure 6. Linear transmission T for a distributed feedback cavity as a function of $k_0 d_n$. The parameters of the cavity are as in figure 1b.

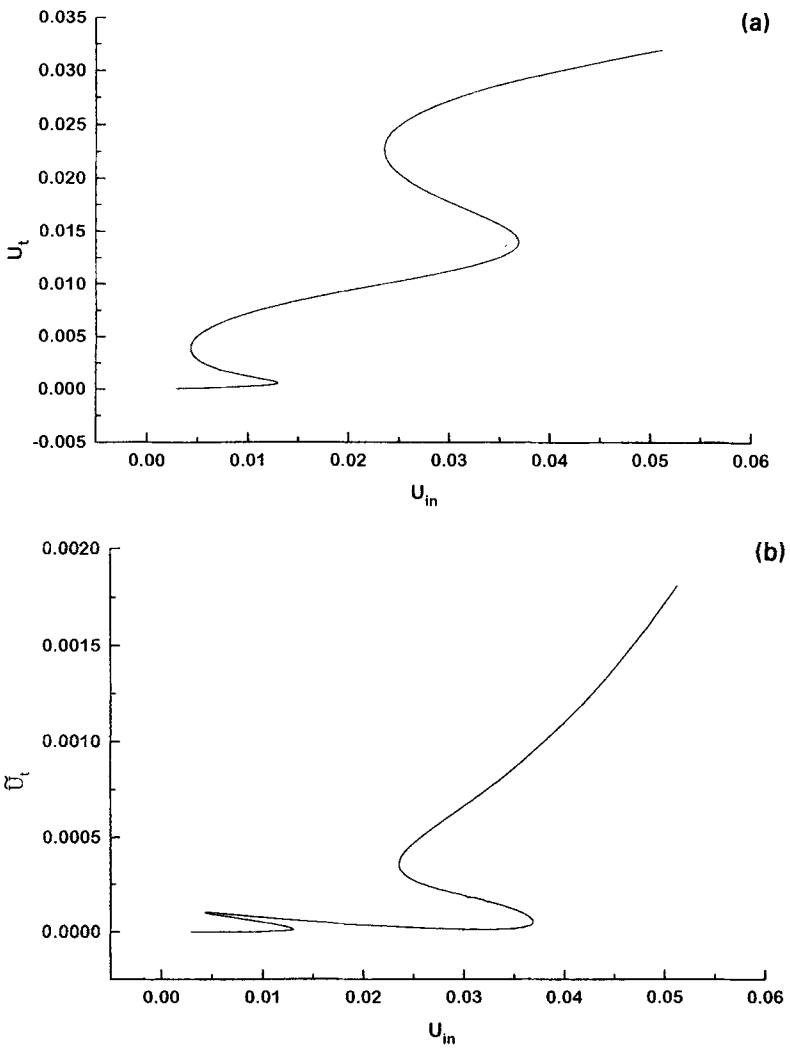

Figure 7. (**a**) U_t and (**b**) $\tilde{U}_t$ as functions of U_{in} for a distributed feedback cavity for $k_0 d_n \sqrt{\varepsilon_n} = 1.391\pi$. The other parameters are as in figure 1b.

fundamental intensity. It can be seen from figure 7 that the features observed for the Fabry–Perot cavity are repeated here.

In both the above cases of Fabry–Perot and distributed feedback cavities we also looked at the reflected fundamental wave as well as the generated third harmonic in the backward direction. They also exhibit bistable response as functions of fundamental intensity and frequency. We do not show those results here.

4. Conclusion

We considered third harmonic generation in layered configurations. We showed that bistability of the fundamental wave can play a crucial role when one tries to enhance the

generated third harmonic using the high quality factor modes of the structure. Moreover, we showed that the bistable response of the fundamental can lead to multivalued nature of the generated third harmonic. Our calculations suggest the possibility of an all optical switch at third harmonic frequency where the fundamental plays the role of the control. In fact, fundamental intensity or its frequency can be used to switch the value of the generated third harmonic.

Acknowledgements

One of the authors (SDG) would like to thank the Department of Science and Technology, Government of India for support. The authors are also thankful to V Mahalakshmi for help in computation.

References

[1] N Bloembergen and P S Pershan, *Phys. Rev.* **128**, 606 (1962)
[2] D S Bethune, *J. Opt. Soc. Am.* **B6**, 910 (1989)
[3] D S Bethune, *J. Opt. Soc. Am.* **B8**, 367 (1991)
N Hashizume, M Ohashi, T Kondo and R Ito, *J. Opt. Soc. Am.* **B12**, 1894 (1995)
[4] D Sarid, *Phys. Rev. Lett.* **47**, 1927 (1981)
S Sarid, R T Deck, A E Craig, R K Hickernell, R S Jameson and J J Fasano, *Appl. Opt.* **21**, 3993 (1982)
G S Agarwal, *Phys. Rev.* **B31**, 3534 (1985)
[5] F S Felber and J H Marburger, *Appl. Phys. Lett.* **28**, 731 (1976)
J H Marburger and F S Felber, *Phys. Rev.* **A17**, 335 (1978)
[6] G S Agarwal and S Dutta Gupta, *Phys. Rev.* **B34**, 5239 (1986)
[7] G S Agarwal and S Dutta Gupta, *Opt. Lett.* **12**, 829 (1987)
[8] S Dutta Gupta, *J. Opt. Soc. Am.* **B6**, 1927 (1989)
[9] M B Pande, Ranjit Singh and S Dutta Gupta, *J. Mod. Opt.* **40**, 901 (1993)
[10] S Dutta Gupta and G S Agarwal, *J. Opt. Soc. Am.* **B4**, 691 (1987)
[11] V Mahalakshmi, Jolly Jose and S Dutta Gupta, *Pramana – J. Phys.* **47**, 317 (1996)
[12] P Yeh (ed.), *Optical waves in layered media* (Wiley, New York, 1988) p. 118
[13] S Dutta Gupta and G S Agarwal, *Opt. Commun.* **103**, 122 (1993)
[14] The concept and implementation of quasi phase matching was developed keeping in view mostly second order nonlinear processes. See, for example, J A Armstrong, N Bloembergen, J Ducuing and P S Pershan, *Phys. Rev.* **127**, 1918 (1962)
J D Bierlein, *Guided wave optics* edited by D B Ostrowsky and R Reinisch (Kluwer Academic, Dordrecht, 1992) p. 49
M M Fejer, *Guided wave optics* edited by D B Ostrowsky and R Reinisch (Kluwer Academic, Dordrecht, 1992) p. 133
M M Fejer, G A Magel, D H Jundt and R L Byer, *IEEE J. Quantum Electron.* **28**, 2631 (1992)
[15] D Williams, D West and T King, presented at the European Quantum Electronics Conference, September 8–13 (Hamburg, Germany, 1996)
[16] M Born and E Wolf, *Principles of optics* (Macmillan, New York, 1965) p. 62